Optical studies in the range 2–9 eV of ion-implanted MgF_2 crystals

A. T. Davidson
Physics Department, University of Zululand, KwaDlangezwa 3886, South Africa

J. D. Comins
Department of Physics, University of the Witwatersrand, P.O. Wits, Johannesburg 2050, South Africa

T. E. Derry
Schonland Research Centre for Nuclear Sciences, University of the Witwatersrand, P.O. Wits, Johannesburg 2050, South Africa

A. M. J. Raphuthi
Physics Department, University of Zululand, KwaDlangezwa 3886, South Africa
(Received 9 September 1992; revised manuscript received 10 March 1993)

MgF_2 crystals have been implanted with 100-keV metallic ions (sodium, magnesium, aluminum) and rare-gas ions (neon, argon, krypton, xenon). Dose levels were in the range $(6–100)\times10^{15}$ cm^{-2}. The nature and thermal stability of the induced defects is discussed. At low dose levels, F and F_2 centers are produced. Coloration is more efficient with metallic ions than with rare-gas ions. In magnesium-implanted crystals, an F band and three F_2 bands (3.91, 3.36, and 3.08 eV) are resolved. A fourth band is present at 2.84 eV and could also be an F_2 band. A band near 5.66 eV is attributed to π-type transitions of the F_2 centers. Extrinsic colloid bands characteristic of the implanted metallic ions form at large doses. An intrinsic magnesium colloid is observed at 4.43 eV in krypton-implanted crystals also at large doses.

I. INTRODUCTION

In this paper we discuss the production of defects in MgF_2 crystals by the process of ion implantation. The work was stimulated by similar experiments on LiF where absorption spectroscopy is used to detect changes resulting from implantation of 100-keV ions.[1] We observe defects at higher concentrations than is normally achieved by other methods of radiation damage. In ion implantation, defects are located primarily within the range of the implanted ions, which here it is only a fraction of a micrometer. Thus the optical thickness of the defect layer is very small, leading to optical-absorption bands which remain readily measurable.

Many workers have reported radiation-induced defects in MgF_2. These include experiments on pure crystals using 1.7-MeV electrons and ^{60}Co γ rays,[2] 50-kV x-rays,[3] 400-keV electrons and 50-kV x-rays,[4] and high-energy protons.[5] More recently, enhanced damage from combined electron-beam and optical excitation has been reported.[6] Doped crystals have been investigated using ^{60}Co γ rays.[7,8] It is now generally recognized that the defect production mechanism is excitonic in nature and is related to that observed in the alkali halides.[6,9,10]

The radiation-induced defects absorbing in the visible region of the spectrum have been identified by Blunt and Cohen,[3] and by Facey and Sibley.[11] The F band occurs near 4.77 eV (260 nm), is slightly anisotropic and is polarization dependent. Four types of F_2 center have been suggested for the rutile structure.[11] The symmetry of two of these has been positively identified by Facey and Sibley,[11] namely $F_2(1)\equiv M(C_{2h})$ at 370 nm and $F_2(2)\equiv M(D_{2h})$ at 320 nm. An additional band $F_2(3)$ has been observed at 400 nm. These transitions yield absorptions at lower energy than the F band; in addition theory predicts the occurrence of π transitions which would be "F like" and close to F-center energies. The relative proportion and distribution of the F and F_2 centers among these possible variants depends on the nature of the irradiation and subsequent bleaching treatments.

This work is concerned with MgF_2 implanted with 100-keV ions Na^+, Mg^+, Al^+, Ne^+, Ar^+, Kr^+, and Xe^+ over a range of doses. This represents a systematic study of ion-implanted samples by optical methods in the visible and vacuum ultraviolet (VUV). A previous investigation by Becher, Kernell, and Reft[5] using 40- and 80-MeV protons has been reported in which F-center absorption was observed at 4.77 eV (260 nm) but little change in the VUV region for the relatively low dose of 8×10^{12} cm^{-2}.

II. EXPERIMENTAL PROCEDURE

Polished plates of thickness 1 mm were obtained from BDH (Merck) in the United Kingdom. Square specimens of side 6 mm were cut with a diamond wire saw. Specimens were implanted with 100-keV ions at the Schonland Research Center for Nuclear Sciences at the University of the Witwatersrand. Unless specified, ions were implanted at ambient temperature without active cooling of the samples during the process. Beam currents were in the range 2–8 μA cm^{-2}. The temperature rise of the crystal surface during implantation can be significant especially at the larger beam currents. For example, during high-dose (10^{17} cm^{-2})argon-ion implantations, we ob-

 ©1993 The American Physical Society

serve that for a beam current of 2.5 μA cm^{-2}, the temperature of the implanted surface reaches 160 °C during the implant. This was measured using a thermocouple attached to the surface of the crystal. For a beam current of 7.5 μA cm^{-2}, the temperature reaches 248 °C. These values are much higher than is observed for the sample holder itself, where a temperature rise of about 30 °C is typical for the above conditions. We have also used a temperature-controlled sample holder which promotes uniform crystal temperature during implantation. This was used for a few selected crystals only. The temperature-controlled sample holder has relatively low thermal inertia and is stabilized by a combination of electrical heating and the flow of liquid nitrogen. No special precautions were taken to prevent charging of the crystals during implantation; however previous experience demonstrated no effects on optical spectra attributable to this effect.[1]

Optical-absorption spectra were obtained in the range 700–200 nm using Beckman Du-8 or Du-70 spectrophotometers. A few spectra were extended into the VUV region. Here we used a Rank Hilger E760 vacuum grating monochromator fitted with a sodium salicylate sensitized EMI 9558B photomultiplier. Our absorbance curves show the defect-induced absorbance with an untreated MgF_2 crystal being used for reference.

Some thermal annealing experiments were performed on crystals after implantation. Selected crystals were isochronally annealed in darkness in air in steps of 50 °C starting from a temperature of 50 °C. The duration of annealing at any specified temperature was 30 min. After each step, the crystal was rapidly cooled to ambient temperature and the absorption spectrum was measured.

III. RESULTS

A. Magnesium-ion implantations

Figure 1 shows absorption spectra obtained for increasing doses of magnesium ions implanted into MgF_2 crystals. Five absorption peaks are resolved which are identified as the F band (4.96 eV, 250 nm) and a cluster of F_2 bands labeled $F_2(1)$ (3.36 eV, 369 nm), $F_2(2)$ (3.91 eV, 317 nm), and $F_2(3)$ (3.08 eV, 403 nm) in order of prominence. It is noted that the F band is asymmetrical having structure $F_2(\pi)$ peaking at 5.66 eV (219 nm) on the high-energy side. This is absent in x-ray-irradiated crystals[3] in which low F_2-center concentrations occur. We thus attribute the structure to π-type optical transitions of the F_2 centers, which would absorb near the F band.

The results of isochronal annealing a crystal implanted with 10^{16} Mg ions cm^{-2} are shown in Fig. 2(a). The F, $F_2(1)$, and $F_2(2)$ bands anneal between 200 and 350 °C. Within this temperature range, a new broad band, C, appears at 4.43 eV (280 nm) in the absorption spectrum. It becomes more prominent as the temperature is raised, reaches a maximum at 550 °C and disappears by about

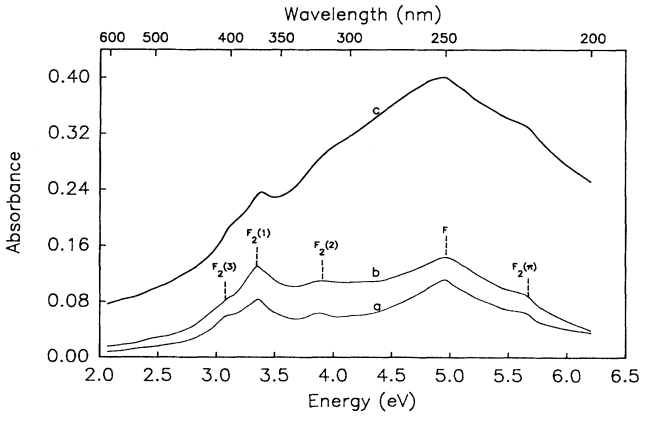

FIG. 1. Absorbance vs photon energy between 2.0 and 6.2 eV for MgF_2 crystals implanted with magnesium ions (100 keV, 2 μA cm^{-2}) at ambient temperature and not actively cooled. The curves correspond to different doses of implanted ions. (a) 6×10^{15} cm^{-2}, (b) 1×10^{16} cm^{-2}, (c) 3×10^{16} cm^{-2}.

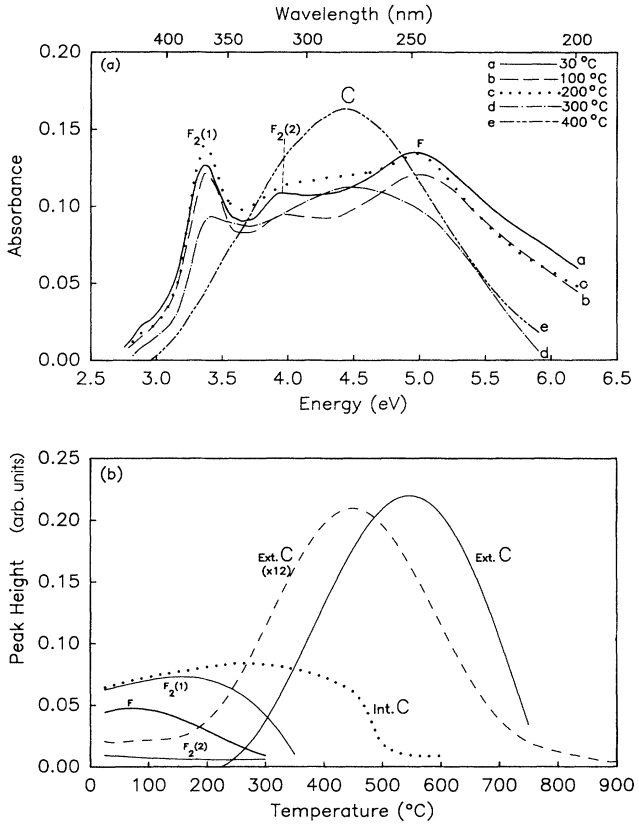

FIG. 2. (a) Annealing behavior of a MgF_2 crystal after implantation with a dose of 10^{16} magnesium ions (100 keV, 2 μA cm^{-2}) at ambient temperature and not actively cooled. The curves show changes in absorbance during an isochronal anneal consisting of 50 °C stages each of duration 30 min. (b) The temperature dependence of the absorption bands shown in Fig. 2(a) for a magnesium-implanted crystal is given by the solid curves. Also shown are growth curves of the extrinsic magnesium colloid (dashed curve, X12) and the intrinsic magnesium colloid (dotted curve) produced by high-dose magnesium and krypton-ion implantations, respectively. Refer to the text for further details.

750 °C as shown by the solid line (Ext. C) in Fig. 2(b).

Implanting a larger dose (8.7×10^{16} cm^{-2}) of magnesium ions produces a band at 5.02 eV (247 nm) which extends over a wide spectral range. This is shown in Fig. 3 together with spectra obtained for crystals implanted with similarly large doses of aluminum and sodium ions. The broad bands in Fig. 3 are colloid bands and will be discussed later. The results of an isochronal anneal of the magnesium colloid band in the crystal shown in Fig. 3, is given in Fig. 4. The band at 5.02 eV grows dramatically and the bandwith decreases as the temperature is raised. The peak absorbance moves to lower energies and stabilizes near 4.34 eV (286 nm) at a temperature of 450 °C. The band decreases on further annealing and disappears by 900 °C. The temperature dependence of this band is included in Fig. 2(b) and is given by the dashed curve marked Ext. C (X12).

B. Aluminum-ion implantations

Figure 5(a) shows absorption spectra obtained for increasing doses of aluminum ions implanted in MgF_2. For comparison purposes, Fig. 5(b) shows spectra for crystals implanted with 10^{16} cm^{-2} aluminum and magnesium ions. We see that the $F_2(1)$ band is more prominent and that the $F_2(2)$ and $F_2(3)$ bands have very low intensities in the aluminum sample. There is extra absorption near 2.84 eV (437 nm) in both spectra shown in Fig. 5(b). We suggest that this is due to the fourth predicted form of the F_2 center; previous investigations have not identified the $F_2(4)$ center owing to low concentrations.

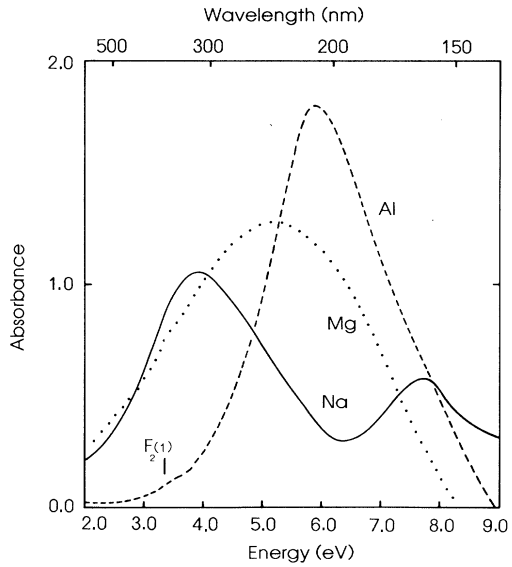

FIG. 3. Absorbance vs photon energy between 2.0 and 9.0 eV of MgF_2 crystals implanted at ambient temperature with 100-keV sodium, magnesium, and aluminum ions to similar large doses. Line curve, sodium ions, 8×10^{16} cm^{-2}; dotted curve, magnesium ions, 8.7×10^{16} cm^{-2}; dashed curve, aluminum ions, 1×10^{17} cm^{-2}. A temperature rise occurred in these crystals during implantation.

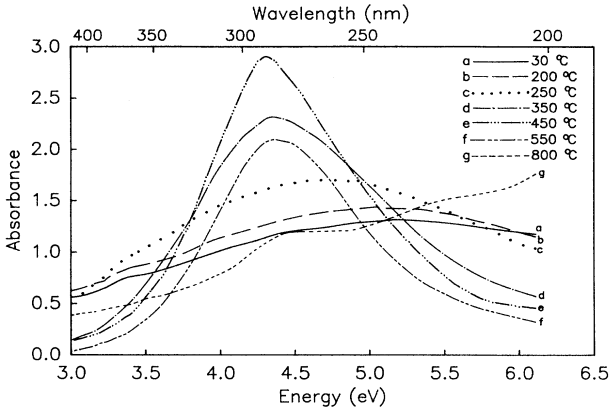

FIG. 4. Annealing behavior of a MgF_2 crystal after implantation with a dose of 8.7×10^{16} cm^{-2} magnesium ions at ambient temperature and not actively cooled. The isochronal anneal consisted of 50 °C stages each of duration 30 min. The curves show changes in absorbance during the isochronal anneal and correspond to annealing temperatures shown.

Annealing experiments undertaken on the crystal implanted with 10^{16} Al ions cm^{-2} showed a similar trend to Fig. 2(a) for magnesium ions, except that the broad band emerged at larger photon energies in the region of 6.2 eV (200 nm). This indicates that an aluminum colloid forms on annealing. The colloid band in aluminum-implanted crystals should not be confused with the $F_2(\pi)$ band, which absorbs in a similar spectral region. The colloid band is already prominent in the spectra of crystal implanted with 3×10^{16} Al ions cm^{-2} in Fig. 5(a). It occurs at 5.90 eV (210 nm) in a crystal implanted with 6×10^{16} Al ions cm^{-2} and at doses of 10^{17} cm^{-2}, the aluminum colloid band dominates the spectrum as shown in Fig. 3.

C. Implants using rare-gas ions

Several MgF_2 crystals were implanted with argon, krypton, and xenon ions at various doses in the range 10^{16} cm^{-2}–10^{17} cm^{-2} at ambient temperature. In these experiments little absorption occurred. In case this result was due to annealing resulting from a significant temperature rise occurring during a high-dose implantation, check experiments were carried out in a special run. Here both MgF_2 and LiF crystals were implanted using the constant temperature sample holder operating at 20 °C. Neon and krypton ions were implanted to a dose of 10^{16} cm^{-2}. Whereas the coloration in the LiF crystal was similar to that reported by us earlier,[1] only small $F_2(1)$ bands were observed in MgF_2; the F band was not obvious.

Small concentrations of color centers were observed in MgF_2 when the much larger dose of 10^{17} Ar ions cm^{-2} was implanted using the constant temperature holder operating at 70 °C. As shown in Fig. 6, absorption bands are present at 5.65 eV [$F_2(\pi)$], 4.76 eV (F), 3.39 eV [$F_2(1)$], 3.84 eV [$F_2(2)$], and 4.13 eV. We note that the energy of the F band shown in Fig. 6 is in good agreement with values given by other workers mentioned in

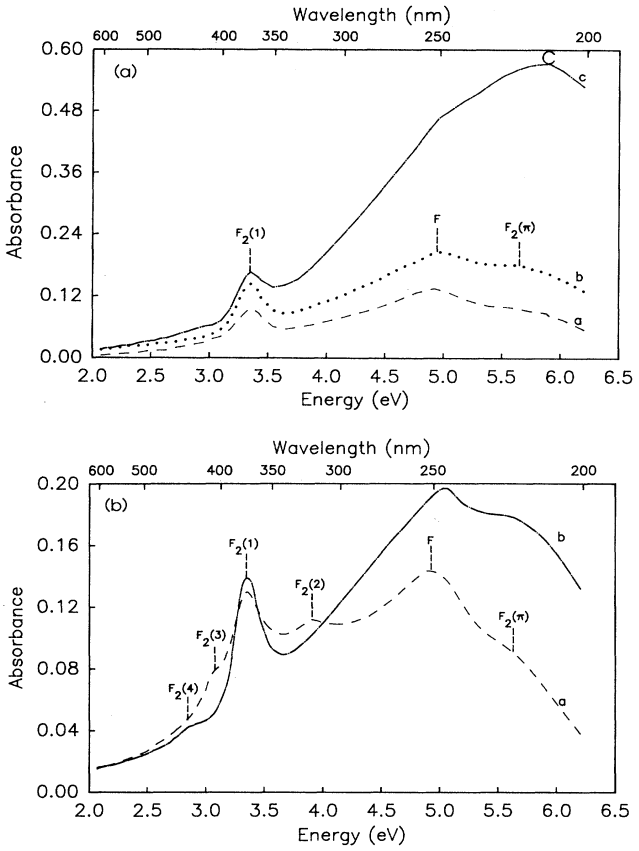

FIG. 5. (a) Absorbance vs photon energy between 2.0 and 6.2 eV for MgF_2 crystals implanted with aluminum ions (100 keV, 2.5 $\mu A\,cm^{-2}$) at ambient temperature and not actively cooled. The curves correspond to different doses of implanted ions. (a) 6×10^{15} cm^{-2}, (b) 1×10^{16} cm^{-2}, (c) 3×10^{16} cm^{-2}. (b) Absorbance vs photon energy between 2.0 and 6.2 eV for MgF_2 crystals implanted at ambient temperature with the same dose, 1×10^{16} cm^{-2}, of 100-keV magnesium (curve a) and aluminum (curve b) ions. The crystals were not actively cooled during implantation.

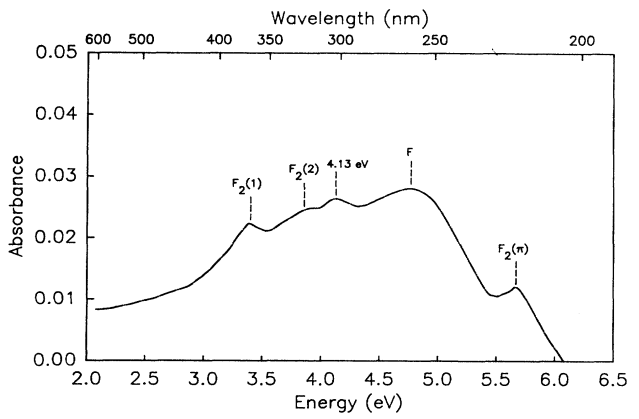

FIG. 6. Absorbance vs photon energy between 2.0 and 6.2 eV for a MgF_2 crystal implanted at a stabilized temperature of 70 °C with 100-keV argon ions. The dose was 1×10^{17} cm^{-2} and the beam current 2 $\mu A\,cm^{-2}$.

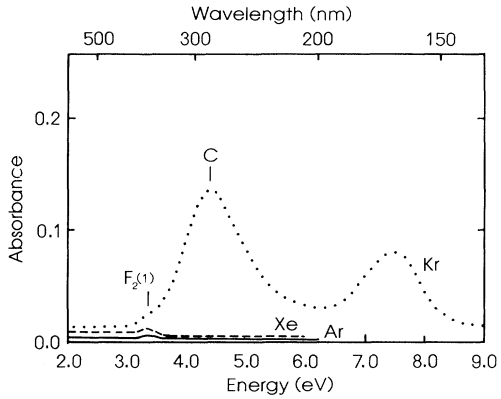

FIG. 7. Absorbance vs photon energy between 2.0 and 9.0 eV for MgF_2 crystals implanted at ambient temperature with similar doses, 1×10^{17} cm^{-2}, of 100-keV rare-gas ions. Dotted curve, krypton ions, beam current 7.5 $\mu A\,cm^{-2}$; dashed curve, xenon ions, beam current 8.0 $\mu A\,cm^{-2}$; line curve, argon ions, beam current 8.0 $\mu A\,cm^{-2}$. A temperature rise occurred in these crystals during implantation.

the Introduction, namely 4.77 eV. In our implantation experiments using magnesium and aluminum ions, the F band occurs at slightly higher energy, namely 4.96 eV. We think that this is due to strong $F_2(\pi)$ absorption in the region of the F band in samples implanted with metallic ions. Accordingly we favor 4.76 eV as the F band energy in MgF_2.

For implantations done with no temperature control, it is only the high-dose implantation with krypton (10^{17} cm^2, 7.5 $\mu A\,cm^{-2}$) which resulted in significant spectral features. As is shown in Fig. 7, a weak band occurs at 4.43 eV (280 nm) in the visible region with a band at 7.25 eV (171 nm) in the VUV. The presence of the band at 4.43 eV was rechecked in a second crystal implanted under similar conditions. During the course of an isochronal anneal, the band at 4.43 eV remained essentially the same until a temperature of 300 °C was reached. Thereafter it decreased slightly until 450 °C and faded rapidly at higher temperatures with the peak energy remaining the same. It disappeared by 600 °C. The VUV region was not monitored during this annealing procedure. We consider that the peak at 4.43 eV in Fig. 7 is an intrinsic magnesium colloid for reasons which will be discussed below. We have only been able to produce it with krypton ions; the other rare-gas ions did not give the same result.

In Fig. 2(b) the annealing behavior of the intrinsic magnesium colloid represented by the dotted curve is compared with that of extrinsic magnesium colloids produced in crystals implanted with magnesium ions.

IV. DISCUSSION

A. Color centers

The degree of coloration of ion-implanted MgF_2 depends strongly on the nature of the implanted ions. Stable defects identified as F and F_2 centers are produced

following implantation with metallic ions such as magnesium and aluminum, but very low coloration is produced by rare-gas ions. Even for the metallic ions used, we find a difference in the type of F_2 center produced. We observe many of the F_2 bands mentioned in the earlier literature and discussed in the introduction in magnesium-implanted crystals, namely the $F_2(1)$ (3.36 eV), $F_2(2)$ (3.91 eV), and $F_2(3)$ (3.08 eV) bands shown in Fig. 5(b). If we include the band at 2.84 eV [$F_2(4)$], which is just resolved in Fig. 5(b) as part of the cluster of F_2 bands, then we have observed four F_2 bands. This is the number expected on theoretical grounds.[11] The $F_2(1)$ band at 3.36 eV is the most prominent and thermally stable of the F_2 bands in crystals implanted with metallic ions. We also consider that we have identified the F-like transition associated with the π orbitals of the F_2 centers; this yields an absorption $F_2(\pi)$ at 5.66 eV. The $F_2(\pi)$ band is well resolved in the spectrum of an argon-implanted crystal shown in Fig. 6. A similar F-band asymmetry, which we attribute to the $F_2(\pi)$ band, is present in previous studies of neutron-irradiated MgF_2 by Facey and Sibley[11] in which large concentrations of F_2 centers were present.

Also resolved in Fig. 6 is an absorption band situated at 4.13 eV (300 nm) between the F and $F_2(2)$ bands. This extra band at 4.13 eV and the $F_2(2)$ band have both been seen in x-irradiated crystals following optical bleaching of the F band.[3] We suggest that the band at 4.13 eV may be due to a higher-order F-center aggregate, such as an F_3 center. We note however, the very low absorbance levels in Fig. 6.

Our observation that metallic ions are considerably more efficient in creating color centers than rare-gas ions of comparable mass and of the same energy in MgF_2, parallels the results obtained by us earlier on ion-implanted LiF crystals.[12] Hence it appears that this is a more universal phenomenon and not restricted to the alkali halides. This very significant difference appears not to be directly related to the electronic or nuclear stopping power as is also indicated by computer simulations. As an illustration, a TRIM-89 (Ref. 13) simulation of recoil distributions and ionization energy loss in MgF_2 for 100-keV rare-gas ions Ne^+ and Ar^+ and for 100-keV metal ions Na^+ and Al^+ was carried out. A comparison of the results for Ne^+ and Na^+, those being of comparable mass, is given in Fig. 8. It shows only a small variation in energy deposition for the two cases. An explanation already suggested in the case of LiF lies in the different chemical nature of the implanted ions. Metal ions are more likely to substitute into the lattice, thereby providing trapping sites for interstitial halogen defects; this would reduce vacancy-interstitial recombination during implantation. Rare-gas ions are likely to produce a separate phase such as internal bubbles or possibly escape from the crystal.

Regarding our explanation for the coloration of MgF_2 by implanted metal ions given above, it is known that metal ions incorporated substitutionally in alkali halides can alter F-center production rates by acting as traps for interstitial halogen defects thereby reducing vacancy-interstitial recombination. The exact location of the metal ions in ion-implanted MgF_2 requires further study, but we consider that similar processes are likely to be operating.

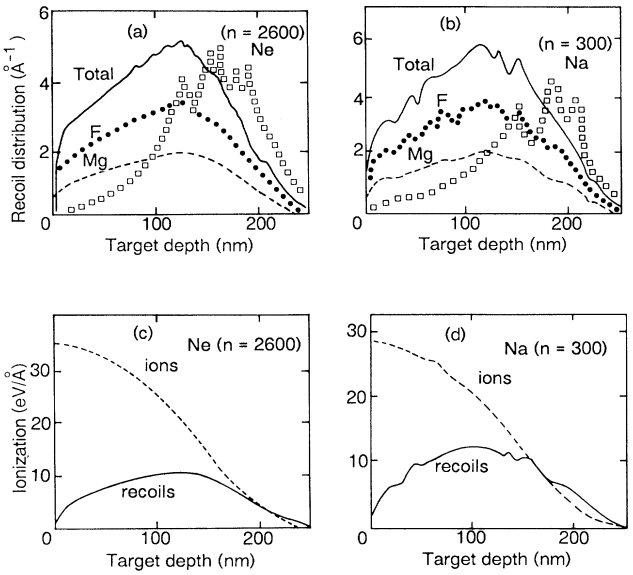

FIG. 8. (a) Results of a TRIM-89 (Ref. 13) calculation showing the distribution of incident ions and recoil ions for collision-induced damage in MgF_2 crystals implanted with 100-keV Ne^{20} ions. (b) The same as (a) for MgF_2 implanted with 100-keV Na^{23} ions. (c) TRIM-89 simulation of the energy loss by ionization for 100-keV Ne^{20} ions in MgF_2 showing relative contributions from the incident and recoil ions. (d) The same as (c) for MgF_2 implanted with 100-keV Na^{23} ions.

B. Colloids

Both extrinsic and intrinsic colloids are observed in ion-implanted MgF_2 crystals. Colloids are small metal particles whose presence is inferred from broad bands in the optical-absorption spectra.[14] Colloid bands for sodium, magnesium, and aluminum are shown in Fig. 3. As expected, the bands move to higher photon energies as the plasmon energy of the metal increases.

Using the simplest theory,[15] assuming spherical particles and ignoring birefringence effects by taking an average crystal refractive index of $n = 1.38$, we have calculated the expected peak positions of the colloid bands for sodium, magnesium, and aluminum in MgF_2. The agreement for "as-implanted" colloids is only fair as shown in Table I. However in the magnesium case, we carried out annealing routines in which the colloid band narrowed and shifted somewhat in spectral position indicating a reduction in the range of sizes and variations in morphology. These anneals result in colloid bands both intrinsic and extrinsic which agree well in spectral characteristics and with the theory. Presumably similar treatments of the sodium and aluminum cases would be necessary to improve experimental and theoretical agreement. In this regard, recent Raman studies in NaCl irradiated by elec-

TABLE I. Peak energy (in eV) of colloid bands observed in ion-implanted MgF_2 crystals. The predicted peak energy of the colloid band ($h\omega_c$) depends on the plasmon energy ($h\omega_p$) and is calculated using $h\omega_c = h\omega_p(1+2n^2)^{-1/2}$.

Ion	$_{11}$Na	$_{12}$Mg	$_{13}$Al
Plasmon energy[a]	5.71	10.6	15.3
$(h\omega_c)_{\text{observed}}$	3.86	5.03[b]	5.80
		4.34[c]	
		4.43[d]	
$(h\omega_c)_{\text{predicted}}$	2.60	4.83	6.98

[a]Values of plasmon energy (in eV) from Ref. 18.
[b]Extrinsic colloid in a Mg implanted crystal.
[c]Extrinsic colloid after the annealing procedure.
[d]Intrinsic colloid in a Kr implanted crystal.

trons to high doses, produced colloids with fractal structures;[16] this morphology is distinctly different from the spherical models usually assumed.

The extrinsic colloid bands discussed above are produced in crystals implanted near ambient temperature with large doses of metallic ions. It is apparent that the temperature rise of the sample during implantation may be promoting the production of these colloids. This is based on observations using the temperature-controlled sample holder, which showed that stabilizing the temperature, T_s, of a crystal during an implantation could effect the colloid bands. In the case of Mg^+ ions implanted to relatively large doses (6×10^{16} cm^{-2}, 2.0 μA cm^{-2}), the colloid band was absent in a crystal implanted with $T_s = 0$ °C but was well developed in a crystal implanted at ambient temperature without active cooling. In a similar experiment using Al^+ ions (6×10^{16} cm^{-2}, 2.5 μA cm^{-2}), the colloid band was present in a crystal implanted with $T_s = -80$ °C but was reduced in size when compared with a crystal implanted at ambient temperature without active cooling. Colloid bands are also produced on annealing MgF_2 crystals implanted with lower doses of metal ions when only F-type defects are present in the spectra initially. We believe that the colloids produced in this case are also extrinsic and arise from the implanted ions. As shown in Fig. 2(a), and by the solid curves in Fig. 2(b), F and F_2 centers anneal during the first stage and is followed by colloid development.

Turning to the rare-gas implantations, we propose by comparison with the extrinsic magnesium colloid band that the weak band at 4.43 eV in the spectra of krypton implanted crystals is due to an intrinsic magnesium colloid. It is not clear at this state why only krypton of the rare gases used is able to produce the colloid. A large ion dose (10^{17} cm^{-2}) at large beam currents (8 μA cm^{-2}) is required. Possibilities to be considered include a dose rate effect, interactions between transient color centers, and heating effects at large beam currents. Up till now, intrinsic colloids have not been reported in MgF_2 crystals,[14] so their observation under the present conditions is of interest. The intrinsic colloids would be expected to result directly from F-center aggregation, while the extrinsic colloids result from the direct agglomeration of the implanted ions.

C. Vacuum ultraviolet spectra

Weak bands are observed in the VUV in crystals implanted with large doses ($>8\times10^{16}$ cm^{-2}) of sodium or krypton ions in our present experimentally accessible range up to 9 eV. This can be seen in Figs. 3 and 7. The bands occurred at 7.85 eV (158 nm) for sodium implants and at 7.25 eV (171 nm) for krypton implants. The responsible defects form in the same high-dose regime as the colloid bands present at lower photon energies. By analogy with our previous LiF work,[1,17] absorption in a similar region is suggested to be due to the presence of molecular fluorine. In the case of LiF, a band is observed at the same energy, namely 8.4 eV, in crystals implanted with high doses ($\sim10^{17}$ cm^{-2}) of argon, magnesium, and sodium ions. For this reason it was assigned to an intrinsic defect with a molecular fluorine phase being preferred. In the present case of MgF_2, absorption is found in a similar region in two implanted crystals and may have a similar origin. No significant defect-induced absorption was found in the VUV for MgF_2 crystals implanted at lower doses.

V. SUMMARY

(a) MgF_2 crystals have been implanted with 100-keV metallic and rare-gas ions near ambient temperature at doses in the range 6×10^{15} cm^{-2}–1×10^{17} cm^{-2}.

(b) At low doses, F-type color center bands characteristic of the host crystal are produced by implanting magnesium and aluminum ions. A variety of F_2 centers is observed owing to the low symmetry of the rutile structure of MgF_2. In addition to the three known F_2 centers, a candidate for the fourth type has been found at 2.84 eV. An $F_2(\pi)$ band is identified at 5.66 eV in this investigation.

(c) In contrast, rare-gas ions of similar stopping power, energy, and fluence as the metal ions in (b) above, color MgF_2 very inefficiently.

(d) Colloid bands are produced following large dose implants of sodium, magnesium, and aluminum ions. Intrinsic magnesium colloids are produced in crystals implanted with krypton ions but not with argon or xenon ions (masses on either side of krypton).

(e) Color centers anneal between 200 and 350 °C in ion-implanted crystals. Intrinsic and extrinsic magnesium colloids anneal at higher temperatures.

ACKNOWLEDGMENTS

A.T.D. thanks Professor B. Spoelstra for continued interest and the Research Committee of the University of Zululand for financial support. A financial allocation from the University Development Programme of the Foundation for Research Development (FRD) is also acknowledged. A.M.J.R. thanks the FRD for financial support. J.D.C. thanks the FRD for research support. At the Schonland Research Centre, we thank Rose Cawood and Shunmugam Naidoo for carrying out the ion implantations, and DeBeers and the FRD for financial assistance.

[1]A. T. Davidson, J. D. Comins, and T. E. Derry, Radiat. Eff. **90**, 213 (1985).
[2]W. A. Sibley and O. E. Facey, Phys. Rev. **174**, 1076 (1968).
[3]R. F. Blunt and M. I. Cohen, Phys. Rev. **153**, 1031 (1967).
[4]M. R. Buckton and D. Pooley, J. Phys. C **5**, 1553 (1972).
[5]J. Becher, R. L. Kernell, and C. S. Reft, J. Phys. Chem. Solids **44**, 759 (1983).
[6]K. Tanimura and N. Itoh, J. Appl. Phys. **69**, 7831 (1991).
[7]K. K. Kim and A. S. Nowick, Phys. Rev. B **18**, 1840 (1978).
[8]W.-Y. Lin, M.-H. Hon, and S.-J. Yang, Mater. Sci. Eng. **92**, 227 (1987).
[9]N. Itoh, Adv. Phys. **31**, 491 (1982).
[10]W. A. Sibley, Nucl. Instrum. Methods Phys. Res. B **1**, 419 (1984).
[11]O. E. Facey and W. A. Sibley, Phys. Rev. **186**, 926 (1969).
[12]J. D. Comins, A. T. Davidson, and T. E. Derry, Defect Diffus. Forum **57-58**, 409 (1988).
[13]J. F. Ziegler, J. P. Biersack, and U. Littmark, *The Stopping and Range of Ions in Solids* (Pergamon, New York, 1985).
[14]A. E. Hughes and S. C. Jain, Adv. Phys. **28**, 717 (1979).
[15]W. T. Doyle, Phys. Rev. **111**, 1067 (1958).
[16]J. R. W. Weerkamp and J. C. Groote, Ph.D. thesis, Rijksuniversiteit Gronigen, Holland, 1990.
[17]A. T. Davidson, J. D. Comins, T. E. Derry, and F. S. Khumalo, Radiat. Eff. **98**, 305 (1986).
[18]C. Kittel, *Introduction to Solid State Physics,* 5th ed. (Wiley, New York, 1976).